Title

Altered neural activity in the 'when' pathway during temporal processing in fragile X premutation carriers.

Authors

Kim, So-Yeon
Tassone, Flora
Simon, Tony J
et al.

Publication Date

2014-03-01

DOI

10.1016/j.bbr.2013.12.044

Peer reviewed

Behavioural Brain Research 261 (2014) 240–248

Contents lists available at ScienceDirect

Behavioural Brain Research

journal homepage: www.elsevier.com/locate/bbr

Research report

Altered neural activity in the '*when*' pathway during temporal processing in fragile X premutation carriers

So-Yeon Kim[a,b,d], Flora Tassone[b], Tony J. Simon[b,d], Susan M. Rivera[a,b,c,*]

[a] Center for Mind and Brain, University of California, Davis, USA
[b] MIND Institute, University of California, Davis, USA
[c] Department of Psychology, University of California, Davis, USA
[d] Department of Psychiatry and Behavioral Sciences, University of California, Davis, USA

HIGHLIGHTS

- Neurotypical adults show greater right TPJ in temporal than in spatial processing.
- The increased right TPJ activation was not found in fragile X premutation carriers.
- Elevated *FMR1* mRNA explained atypical right TPJ activity in the premutation group.

ARTICLE INFO

Article history:
Received 23 September 2013
Received in revised form
11 December 2013
Accepted 23 December 2013
Available online 5 January 2014

Keywords:
Spatiotemporal processing
Working memory
Fragile X premutation
FMR1 gene
Temporoparietal junction
When pathway

ABSTRACT

Mutations of the fragile X mental retardation 1 (*FMR1*) gene are the genetic cause of fragile X syndrome (FXS). Large expansions of the CGG repeat (>200 repeats) consequently result in transcriptional silencing of the *FMR1* gene and deficiency/absence of the *FMR1* protein (FMRP). Carriers with a premutation allele (55–200 of CGG repeats) are often associated with mildly reduced levels of FMRP and/or elevated levels of *FMR1* mRNA. Recent studies have shown that infants with FXS exhibit severely reduced resolution of temporal attention, whereas spatial resolution of attention is not impaired. Following from these findings in the full mutation, the current study used fMRI to examine whether premutation carriers would exhibit atypical temporal processing at behavioral and/or neural levels. Using spatial and temporal working memory (SWM and TWM) tasks, separately tagging spatial and temporal processing, we demonstrated that neurotypical adults showed greater activation in the '*when* pathway' (i.e., the right temporoparietal junction: TPJ) during TWM retrieval than SWM retrieval. However, premutation carriers failed to show this increased involvement of the right TPJ during retrieval of temporal information. Further, multiple regression analyses on right TPJ activation and *FMR1* gene expression (i.e., CGG repeat size and *FMR1* mRNA) suggests that elevated *FMR1* mRNA level is a powerful predictor accounting for reduced right TPJ activation associated with temporal processing in premutation carriers. In conclusion, the current study provides the first evidence on altered neural correlates of temporal processing in adults with the premutation, explained by their *FMR1* gene expression.

1. Introduction

The ability to mentally represent and process temporal information accurately is an essential component of cognitive functioning in everyday life. For example, when executing a familiar sequence of events, such as assembling a sandwich or paying a bill, organizing and remembering the temporal order of the required actions is critical to complete the task accurately and efficiently. Even something as simple as remembering one's phone number, requires processing of temporal information. Despite its central role in everyday life, it is only recently that researchers have investigated the development of, and neural mechanisms involved in, temporal processing in humans.

With regards to the development of temporal processing, Farzin et al. (2011) recently reported reduced temporal resolution of visual attention in infants compared to that of adults [1]. Specifically, temporal frequency thresholds were measured in infants (6–15 months) using a flicker task. It was found that the temporal resolution of infants was significantly coarser (up to 1 Hz) than that of adults (up to 10 Hz) previously reported [2,3]. Further, atypical development of temporal processing in young children with fragile X syndrome (FXS) was also investigated [4].

* Corresponding author at: Center for Mind and Brain, University of California, Davis, 267 Cousteau Place, Davis, CA 95618, USA. Tel.: +1 530 747 3802; fax: +1 530 297 4603.
E-mail address: srivera@ucdavis.edu (S.M. Rivera).

0166-4328/$ – see front matter © 2014 Elsevier B.V. All rights reserved.
http://dx.doi.org/10.1016/j.bbr.2013.12.044

FXS is the most common form of inherited intellectual disability, which results from large expansions of the CGG trinucleotide repeat in the promoter region of the fragile X mental retardation 1 (*FMR1*) gene located at Xq27.3. When CGG repeat size exceeds 200, silencing of the gene occurs, resulting in reduction or absence of the gene's protein product (fragile X mental retardation 1 protein: FMRP). When CGG repeat sizes range between 55 and 200 (1 of 130–250 females and 1 of 250–800 males; [5]), the gene is unmethylated, but these so-called "premutation carriers" are often associated with mildly reduced levels of FMRP and/or elevated levels of *FMR1* mRNA [6–9]. Individuals with the fragile X premutation are also associated with the risk of developing a late-onset neurodegenerative disorder known as fragile X-associated tremor/ataxia syndrome (FXTAS) [10,11]. Using crowding and flicker tasks, which measured resolution of spatial and temporal visual attention, respectively, Farzin and colleagues (2011) demonstrated that infants with FXS showed greatly reduced resolution of temporal attention (up to 0.5 Hz) compared to their typically developing counterparts. By contrast, the resolution of their spatial attention was not different. Further, the researchers found that the coarse resolution of temporal attention was genetically dosage sensitive such that greater CGG repeat length was associated with lower temporal resolution in infants with FXS. Such findings of impaired temporal processing in infants with FXS have implications on their later development of visual functions that require precise temporal sensitivity, such as motion perception, visual tracking, and memory for temporal order.

The above-mentioned findings of impaired temporal processing in infants with FXS is also in line with recent findings from animal studies using CGG knock-in (KI) mice modeling the FX premutation. Specifically, using a temporal ordering of spatial locations task, Borthwell and colleagues (2012) have found that female CGG KI mice showed reduced spatial and temporal resolution, and the impairment was *FMR1* genetic dosage sensitive indexed by the CGG repeat size [12]. Similarly, Hunsaker et al. (2010) also demonstrated that female KI mice with higher CGG repeat expansions (i.e., 150–200 repeats) performed more poorly on a task for temporal order memory than wildtype mice, whereas those with lower repeat expansions (80–100 CGG) performed similarly to wildtype mice [13]. Further, using tasks requiring spatial and temporal pattern separation, the researchers demonstrated that CGG repeat length negatively modulated spatiotemporal attention in male CGG KI mice [14].

Despite evidence of impaired spatiotemporal processing in CGG KI mice which models possible impairments in spatial and/or temporal functions in individuals with the FX premutation, there are currently no studies that have examined the extent of impairments in temporal processing in carriers with the fragile X premutation either at the behavioral or the neural level. Instead, recent studies have reported impairments in visuospatial processing in adults with the FX premutation without FXTAS (i.e., asymptomatic adults with the FX premutation) [15–18]. In particular, Keri and Benedek [15,16] reported that adults with the FX premutation revealed subtle impairments on tests requiring magnocellular visual pathways projecting to cortical areas responsible for motion perception and visuospatial processing (dorsal occipito-parietal stream). Specifically, adults with the premutation performed a visual contrast sensitivity task consisting of two types of vertical sinusoidal luminance contrast gratings. The two types of gratings had different spatiotemporal properties to bias information processing toward the M (magnocellular) and P (parvocellular) pathways (M pathway: low spatial/high temporal frequency; P pathway: high spatial/low temporal frequency). Using such stimuli, the authors found that premutation carriers had lower contrast sensitivity than controls in the M pathway condition, but not in the P pathway condition, indicating subtle impairments in motion and visouspatial processing in premutation carriers. Furthermore, Hocking and colleagues [17] demonstrated that asymptomatic male premutation carriers with high CGG repeat sizes ($100 < CGG < 200$) performed significantly worse than normal controls on a Dot test of visuospatial working memory (WM). However, notwithstanding evidence of atypical temporal resolution in infants with FXS and findings in CGG KI mice of impairments in temporal order memory, impairments in temporal processing in individuals with the FX premutation remain unspecified.

Thus, in the current study, we investigated whether temporal processing is impaired in asymptomatic adults with the FX premutation at behavioral and/or neural levels. Specifically, we investigated neural correlates associated with temporal processing in neurotypical adults, and examined whether adults with the FX premutation show atypicality in recruiting those regions to process temporal information. Recently, lesion and transcranial magnetic stimulation (TMS) studies provide evidence that the right parietal lobe, especially the right temporoparietal junction (TPJ), plays a core role to process temporal information required in temporal order judgment (*when* pathway; [19–22]). Hence, in the present study, we examined whether activation in the right TPJ associated with temporal processing is significantly reduced in asymptomatic adults with the FX premutation compared to their neurotypical counterparts.

To identify neural regions specifically involved in temporal processing, we developed two WM tasks, namely a spatial WM (SWM) and a temporal WM (TWM) task. The two tasks have identical stimuli and procedures, but the task requirement for each task was different: the SWM task required memory for spatial location, whereas the TWM task required memory for temporal order. Using fMRI and the two WM tasks, we tested the following hypotheses in the current study. First, we hypothesized that neurotypical adults without the premutation allele (i.e., controls) would activate the *when* pathway, namely the right TPJ, to a greater extent during retrieval of temporal order information than spatial location (i.e., in the contrast of TWM retrieval > SWM retrieval). Further, we hypothesized that FX premutation carriers would show attenuated activity in the right TPJ than the controls in the same contrast of interest. Finally, we expected to find a dosage response of *FMR1* gene expression in the FX premutation group, indexed by CGG repeat expansion and/or *FMR1* mRNA level, such that right TPJ activation associated with temporal processing would be significantly accounted for by the degree to which the *FMR1* gene is behaving normally.

2. Methods

2.1. Participants

Twenty asymptomatic young adults with the premutation (premutation group; mean age: 30.4 years, SD = 7.32; Female: 10) and 20 neurotypical, age-matched controls (control group; mean age: 29.7 years, SD = 6.07; Female: 10) with normal or corrected-to-normal vision participated in the current study. Allele status was confirmed by *FMR1* DNA testing. Full-scale IQ (FSIQ) was obtained using the Wechsler Adult Intelligence Scale, third edition (WAIS-III; [23]). Two male participants in the premutation group and 2 female participants in the control group were excluded from further analyses due to excessive movement (>3 mm in x, y, or z planes) during the task in the MRI scanner. As presented in Table 1, the two groups did not significantly differ in age ($t(34) = .11$, $p = .92$), FSIQ ($t(28) = 1.30$, $p = .20$), nor gender ($\chi^2 = .44$, $df = 1$, $p = .51$), but significantly differ in *FMR1* gene expressions: the premutation group showed increased CGG repeat size ($t(21.3) = 12.5$, $p < .001$) and elevated *FMR1* mRNA level ($t(18.9) = 7.5$, $p < .001$) compared to the control group. The two molecular variables showed a significant

Table 1
Group demographic and FMR1 data.

	Control			Premutation			
	N	Mean	Range	*N*	Mean	Range	*t* (*p*)
Age	18	29.9 (6.3)	18–40	18	29.7 (6.8)	18–42	.107 (.92)
CGG repeat size	16	30.3 (7.1)	20–47	18	95.8 (20.9)	60–146	12.5 (<.001)*
FMR1 mRNA	16	1.3 (0.2)	0.9–1.7	17	2.7 (0.7)	1.9–4.6	7.5 (<.001)*
FSIQ	15	119.5 (12.9)	100–140	15	115.5 (12.5)	77–134	1.3 (.20)

Numbers in parenthesis indicate standard deviation.
* Indicates significant mean differences between the two groups.

and positive correlation ($r = .54$, $p = .024$) in the premutation group as found in previous research [8,24,25]. The Institutional Review Board at the UC Davis approved the experimental protocol. Prior to the experiment, each participant provided informed written consent and all were compensated $30 for participation in the MRI scan. Screening for MR safety was also completed on the day of scanning to ensure eligibility for MR. None of the participants was taking psychotropic medications or medications known to affect MR signal.

2.2. Molecular genetics measures

Genomic DNA was isolated from peripheral blood lymphocytes using standard methods (Puregene Kit; Gentra Inc.). CGG sizing and methylation status were assessed by Southern blot and polymerase chain reaction (PCR) analyses. Analysis and calculation of the repeat size were carried out using an Alpha Innotech FluorChem 8800 Image Detection System (for more details, please see [26]). As previously described [24], all quantifications of *FMR1* mRNA were performed using a 7900 Sequence detector (Applied Biosystems).

2.3. Working memory (WM) tasks and statistical analyses

All participants performed two different WM tasks in the scanner: spatial WM (SWM) and temporal WM (TWM) tasks. Each trial in both WM tasks consisted of three phases: encoding (4 s), rehearsal (10 s), and retrieval (4 s). The retrieval phase was followed by a 12 s inter-trial interval (ITI: baseline). The duration of each phase was chosen based on previous fMRI studies with WM tasks [27–29]. In the encoding phase of the SWM task, participants saw four red stars and eight white stars and were asked to memorize locations of the four red stars (Fig. 1A). During the rehearsal phase, a black crosshair was centrally presented on the screen, and participants were instructed to covertly rehearse the four positions of the red stars across the 10 s delay period. In the retrieval phase, participants saw the same array of the 12 stars as in the encoding phase, but this time, only one star was colored yellow (a probe). Participants were asked to judge whether the probe was located in one of the four locations previously occupied with the red stars. After the star array disappeared, a black central crosshair was presented for 12 s (ITI), and participants were

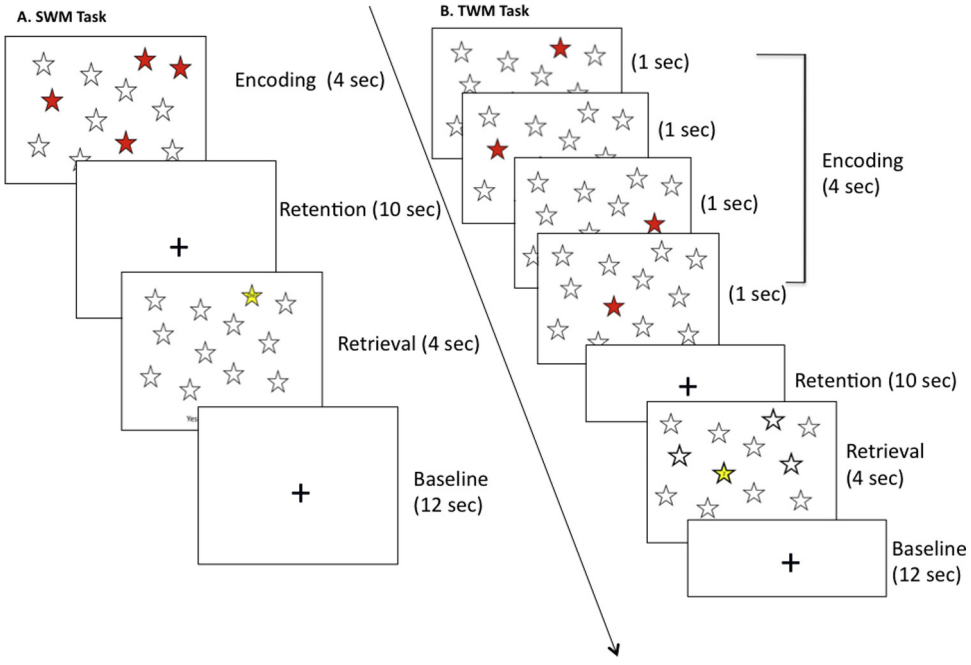

Fig. 1. (A) Trial sequence in the spatial working memory (SWM) task. In the encoding phase, participants saw four red stars and eight white stars for 4 s. Participants were instructed to remember the four positions occupied with the red stars. After the stars disappeared, participants saw a central fixation cross for 10 s (the retention phase). During the retention period, participants were instructed to look at the fixation cross while covertly rehearse the four previously occupied location. After the retention phase, the twelve stars re-appeared with one star was colored yellow (a probe). Participants were asked to judge and respond whether the location of the probe was preoccupied with one of the red stars in the encoding phase. Participants had 4 s to respond, and then, they saw a central fixation cross for 12 s until the next trial begins. (B) Trial sequence in the temporal working memory (TWM) task. In the encoding phase, participants were presented with 12 stars in each trial, but in this task one of the stars was colored red and it changed its location every second during 4 s. Participants were asked to encode the order of the four positions of the red star in each trial. During the retention period, participants were asked to look at the central fixation cross while covertly rehearse the temporal order of the previous four positions with red stars. In the retrieval phase, 12 white stars reappeared and one of them was colored yellow with a number (one, two, three, or four) superimposed on top. Participants were asked to judge whether the number on the star matched to the correct serial position in which it had appeared. The timing of the each phase was identical to those in the SWM task. (For interpretation of the references to color in this legend, the reader is referred to the web version of the article.)

asked to passively look at the fixation cross during this interval.

In the TWM task, participants were also presented with 12 stars in each trial, but in this task one of the stars was colored red and it changed its location every second during the four-second encoding period (Fig. 1B). Participants were asked to encode the order of the four positions of the red star in each trial. In the 10 s of rehearsal phase, the black central crosshair was also presented, but in the TWM task, participants were instructed to covertly rehearse temporal order of the four red stars. In the retrieval phase, 12 white stars reappeared and one of them was colored yellow with a number (one, two, three, or four) superimposed on top. To minimize loads for processing spatial information, previously occupied locations with the red star were indicated with bolded lines. Participants were asked to judge whether the number on the star matched to the correct serial position in which it had appeared. After the retrieval phase, the central fixation reappeared and participants were asked to passively look at the crosshair until the next trial began. Participants performed two runs of each task and each run consisted of 12 trials of memory task lasting for 6 min and 12 s. Before the first run of each task, participants were given two practice trials of each task inside of the scanner.

To test performance differences in spatial and/or temporal WM tasks between the two diagnostic groups, two 2 (WM task, within-subjects factor) × 2 (group, between-subject factor) mixed analyses of variance (ANOVA) were conducted on accuracy and reaction times (RT) data on the two WM tasks. Once significant interaction was detected, paired *t*-tests were performed in each diagnostic group to search for the origin of the interaction. Finally, to examine effects of *FMR1* gene expression (i.e., CGG repeat size and *FMR1* mRNA level) on behavioral performance in each WM task, correlation analyses were conducted between each behavioral data and each molecular variables in each group. All of the statistical analyses on demographic and behavioral performance data were conducted using IBM SPSS statistics 20 (http://www.ibm.com/software/analytics/spss/products/statistics).

2.4. Imaging methods and analyses

2.4.1. Brain image acquisition

All imaging data were acquired on a Siemens 3T Trio scanner with Echospeed gradients and a Siemens 32-channel whole head coil located at the UC Davis Imaging Research Center. Visual stimuli were projected onto a screen and viewed on an MR compatible mirror mounted above the participant's head. For each participant, an anatomical scan was acquired using a high resolution T1-weighted MPRAGE sequence (TR = 2500 ms, TE = 4.33 ms, flip angle = 7°, FOV = 243 mm × 243 mm, 208 slices, 0.95 mm slice thickness). After the anatomical scan, two functional runs were acquired for each participant. For the functional runs, imaging was performed using a T2*-weighted gradient echo planar pulse sequence (TR = 2000 ms, TE = 25 ms, flip angle = 90°). Each brain volume was composed of 36 axial slices (FOV = 220 × 220, matrix = 64 × 64, 3.4 mm × 3.4 mm × 3.4 mm resolution) aligned to the AC–PC line, collected interleaved, inferior to superior. For all functional runs, data from the first two volumes were discarded to allow for stabilization of magnetic fields.

2.4.2. Image processing and fixed-effects analysis

Imaging data were analyzed using SPM 5 (Wellcome Department of Cognitive Neurology, London) run within Matlab (Matlab Mathwork, Inc., Natick, MA). For preprocessing, data were slice-time corrected for acquisition order, realigned and unwarped to correct for motion across runs. Then, the images of each participant were coregistered to their anatomical image. Next, the images were spatially normalized (with trilinear interpolation and preserving the intensities of the original images) to the SPM EPI template corresponding to the MNI (Montreal Neurological Institute) defined standardized brain space, and spatially smoothed with a Gaussian kernel of 5 mm FWHM. Motion estimates were not included as covariates for the fMRI data analysis because all participants who were included in the analyses moved less than 3 mm in *x*, *y*, or *z* planes. The time series were high pass filtered at 128 s.

Statistical analyses were performed using a general linear model for event-related designs in SPM 5 to estimate cortical activation at each memory stage (encoding, rehearsal, and retrieval). For each participant, a whole-brain voxel-wise analysis was conducted in which individual events were modeled as a canonical hemodynamic response. In a fixed effects analysis for each participant, task-related activation in each WM task was modeled using 5 separate regressors for encoding, early rehearsal, late rehearsal, retrieval, and ITI (baseline), each of which was set at 0 s, 6 s, 10 s, 14 s, and 18 s with reference to the onset of each trial, respectively. At these time points, the canonical hemodynamic response function was convolved with a boxcar function with a length of 2.5 s. Such statistical model was selected following previous fMRI studies with WM [27–29]. Specifically, we included separate regressors for early and late rehearsal because the early rehearsal phase was contaminated with activation induced by the sensory stimulation at the encoding phase, thus was not assumed to be independent from the encoding phase [30]. The resulting least squares parameter estimates of the height of the modeled hemodynamic response for each condition were then entered into random effects analyses.

2.4.3. Random effects analyses

The main purpose of the current study was to identify neural correlates of temporal processing and to test whether the neural correlates of temporal processing is altered in adults with the FX premutation. To identify brain areas associated more strongly with temporal processing than with spatial processing, we focused our fMRI analysis on the contrast of TWM retrieval > SWM retrieval. As described above, all the stimuli and procedures in the retrieval phase of the two WM tasks were identical except for the information participants had to retrieve. Specifically, the TWM task requires retrieval of temporal order information, whereas the SWM task requires retrieval of spatial information only. Thus, the results from the contrast of TWM greater than SWM provide us neural regions more strongly associated with temporal than with spatial processing. To determine the presence of significant clusters of activation in the contrast of interest, the joint expected probability distribution method [31] was used yielding a clusterwise significance level of $p < .05$, corrected for multiple comparisons. Group statistical maps were generated using a one-sample *t*-test for each group (height threshold $z > 2.33$, $p < 0.01$, at least 200 consecutive voxels), and group contrast maps were generated using a two-sample *t*-test (height threshold $z > 1.96$, $p < 0.05$, at least 1000 consecutive voxels).

Following the group comparison analysis, regions of interest (ROIs) were defined by the 4-mm-radius sphere around the maxima in each cluster found in the group contrast map to ascertain whether the significant activation in the *when* pathway (i.e., right TPJ) found in the group contrast map was driven by expected interaction effect between diagnostic group and WM task. Beta values of each ROI were extracted from each contrast of "SWM retrieval > Baseline" and "TWM retrieval > Baseline" in each individuals. The extracted beta values were then entered and analyzed in SPSS 20.0 for 2 (WM task) × 2 (group) mixed ANOVAs. Finally, a multiple regression analysis was conducted to examine the relative contributions of CGG repeat size and *FMR1* mRNA level on the *when* pathway for temporal order processing in the premutation group. For each premutation carrier, parameter estimates (beta coefficients) were extracted from the previously defined ROI

in the contrast of TWM > SWM retrieval. Then, a multiple regression analysis was conducted using the beta coefficient as a dependent variable and participant's CGG repeat size and *FMR1* mRNA level as predictors. For correlation analyses, alpha level was corrected for multiple comparison. Test of multicollinearity in the multiple regression analysis did not indicate significant multicollinearity between the two molecular factors (tolerance = .70, VIF (Variance Inflation Factor) = 1.42), justifying the multiple regression analysis with the two molecular variables.

3. Results

3.1. Behavioral performance

Mean accuracy and reaction times (RT) data on each WM task in each diagnostic group are presented in Table 2. Results from the 2 × 2 mixed ANOVA on the accuracy data showed marginally significant main effect of the WM task ($F(1,34) = 3.99$, $p = .054$), resulting from lower accuracy in the SWM than TWM task in both groups. Neither a main effect of group nor an interaction between the two factors was significant (all $p > .05$). Finally, there was no significant correlation between *FMR1* gene expression (i.e., CGG repeat size or *FMR1* mRNA) and accuracy in either group (all $p > .05$).

Results from the same 2 × 2 mixed ANOVA on RT data showed a significant main effect of the WM task ($F(1,34) = 19.43$, $p < .001$), as well as a significant interaction between the WM task and group ($F(1,34) = 7.35$, $p = .01$). A main effect of the group was not significant ($F(1,34) = 2.40$, $p = .13$). Post hoc *t*-tests indicated that the significant main and interaction effects were driven by significantly slower RT in the TWM than the SWM task in premutation carriers (mean differences (MD) = 289 ms, $t(17) = 4.79$, $p < .001$), suggesting relative inefficiency in retrieving temporal order information in individuals with the premutation. RTs in the two WM tasks were not significantly different in the NT group (MD = 46 ms, $t(17) = 1.27$, $p = .22$). Unlike in the accuracy data, we found a significant correlation between RT in the SWM task and *FMR1* mRNA level ($r = .485$, $p = .048$) and a marginally significant correlation between RT in the TWM task and *FMR1* mRNA level ($r = .479$, $p = .052$) in the premutation group only, indicating that premutation carriers with elevated mRNA values tended to take longer time to retrieve spatial and temporal order information than those with lower mRNA levels. Finally, no significant correlation was found between RT data in either WM task and CGG repeat size in either diagnostic group (all $p > .05$).

3.2. Functional imaging results

3.2.1. Group analyses

As shown in Table 3, the control group showed significant activation in bilateral precuneus encompassing bilateral cuneus and cingulate gyrus in the contrast of TWM retrieval > SWM retrieval. Further, we found significantly activated clusters in left inferior parietal lobule (IPL) including left angular gyrus, middle and superior temporal gyrus, and supramarginal gyrus. Finally, the control group also revealed significant activation in right supramarginal gyrus encompassing right superior and middle temporal gyrus,

Table 2
Mean accuracy and response times for each WM task in each group.

	Control		Premutation	
	Accuracy (% correct)	Reaction time (ms)	Accuracy (% correct)	Reaction time (ms)
SWM	90.3 (11.3)	1792 (328)	86.6 (8.8)	1837 (404)
TWM	94.0 (6.3)	1860 (299)*	89.8 (6.9)	2126 (244)*

Numbers in parenthesis indicate standard deviation.
* Indicates significant mean differences between the two groups.

Table 3
Brain areas that showed significant activation in TWM > SWM in each group.

Group	Brain regions	No. of voxels in cluster	Peak coordinates	*t*-Value	Corrected *p*-value of cluster
Control	R precuneus	1352	12 −56 36	5.76	<.001
	L precuneus		−10 −58 30	4.81	
	L cuneus		−4 −82 8	4.27	
	R cuneus		14 −78 32	4.23	
	L cingulate gyrus		−12 −54 28	4.03	
	R cingulate gyrus		14 −36 28	3.66	
	L inferior parietal lobule	1308	−56 −40 42	5.56	<.001
	L angular gyrus		−40 −60 30	5.46	
	L middle temporal gyrus		−38 −60 22	5.45	
	L supramarginal gyrus		−56 −50 34	5.07	
	L superior temporal gyrus		−50 −56 16	4.69	
	R supramarginal gyrus	487	56 −46 38	5.53	<.001
	R superior temporal gyrus		58 −58 14	5.04	
	R middle temporal gyrus		50 −60 22	4.55	
	R temporoparietal junction		52 −38 26	4.15	
	R inferior parietal lobule		54 −42 46	3.64	
	R angular gyrus		48 −68 34	3.64	
Premutation	L superior temporal gyrus	510	−54 −60 28	4.29	<.001
	L angular gyrus		−54 −66 34	4.16	
	L supramarginal gyrus		−42 −52 30	4.1	
	L inferior parietal lobule		−42 −66 44	3.91	
	L superior parietal lobule		−36 −68 44	3.68	
	L middle temporal gyrus		−50 −74 18	3.67	
	L precuneus		−40 −74 34	3.4	

All clusters significant at $p < .05$ corrected.

Table 4
Brain areas that showed greater activation in the control group than the premutation group.

Contrast	Brain regions	No. of voxels in cluster	Peak coordinates	*t*-Value	Corrected *p*-value of cluster
TWM ≥ SWM	R temporoparietal junction	2545	52 −38 22	4.58	<.001
	R supramarginal gyrus		64 −26 40	3.52	
	R inferior parietal lobule		64 −32 38	3.48	
	R superior parietal lobule		32 −60 60	3.38	
	R insula		28 −30 18	3.37	
	R posterior cingulate		48 −24 52	3.13	
	R caudate		20 −2 20	2.95	
	R superior temporal gyrus		42 −40 16	2.78	
	R thalamus		16 −22 6	2.76	
	R precuneus		14 −52 38	2.75	
	R inferior parietal lobule		58 −26 24	2.74	
	L posterior cingulate	2291	−14 −52 8	4.03	<.001
	L thalamus		−24 −24 4	3.61	
	L parahippocampal gyrus		−36 −30 −16	3.59	
	L parahippocampal gyrus/hippocampus		−24 −28 −20	3.27	
	L insula		−40 −20 8	3.16	
	L superior temporal gyrus		−60 −4 −2	3.12	
	L middle temporal gyrus	2660	−36 −58 22	3.22	<.001
	L postcentral gyrus		−38 −26 42	3.06	
	L precentral gyrus		−44 −16 60	3.01	
	L inferior parietal lobule		−42 −26 28	3.01	
	L supramarginal gyrus		−36 −50 26	2.88	
	L precuneus		−8 −38 46	2.59	
	L insula		−34 −8 22	2.55	

All clusters significant at $p < .05$ corrected.

temporoparietal junction (TPJ), IPL, and angular gyrus. Unlike the control group who showed bilateral parietal activation including the right TPJ in the contrast of TWM > SWM retrieval, the premutation group revealed a significant cluster in the same contrast only in the left superior temporal gyrus covering the left angular gyrus, supramarginal gyrus, IPL, middle temporal gyrus, and precuneus (Table 3). It is worth noting that the *when* pathway, including the right TPJ, angular gyrus, supramarginal gyrus and posterior superior temporal gyrus, was significantly activated only in the control group in our contrast of interest, which targeted the neural regions specifically associated with temporal processing.

To test group differences in activation of the *when* pathway, a two-sample *t*-test was conducted on the contrast of TWM > SWM retrieval. Results from the group comparison analysis showed significant activation in the right TPJ in the contrast of Control > Premutation, where the activation extended to the right supramarginal gyrus, superior parietal lobule, insula, superior temporal gyrus, and IPL (Table 4). In the same contrast, we also found significant clusters in the left posterior cingulate, encompassing the left thalamus, parahippocampal gyrus, and insula, and in the left middle temporal gyrus, including the left post- and precentral gyrus, IPL, and precuneus.

Results from the 2 (WM task) × 2 (group) mixed ANOVAs conducted on the beta coefficient values in the significant clusters found in the group contrast map, namely in the right TPJ, left posterior cingulate, and left middle temporal gyrus, supported our hypothesis. As shown in Fig. 2, a significant interaction was observed between WM type and diagnostic group on the right TPJ activation, $F(1,34) = 5.96$, $p = .020$, while main effects of the two factors were not significant (all $p > .05$). Post hoc *t*-tests confirmed

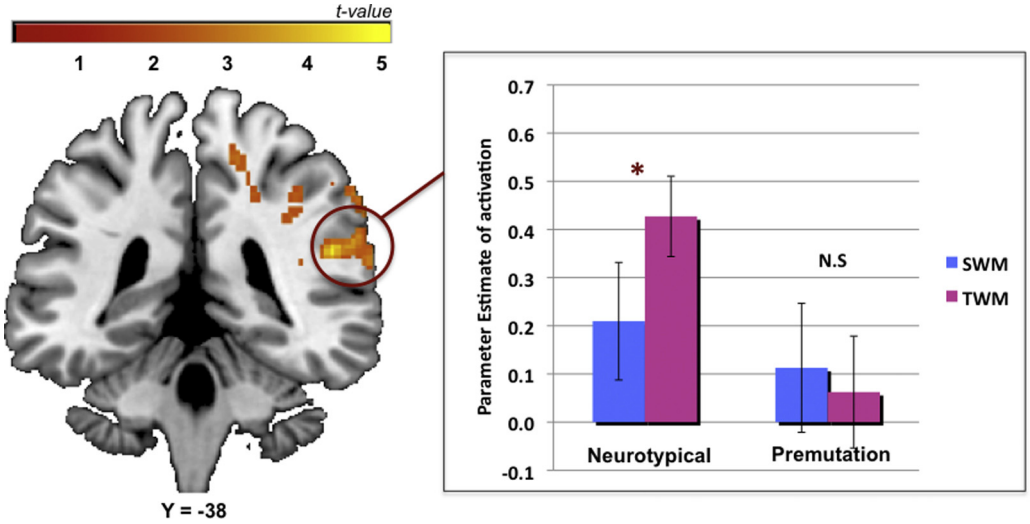

Fig. 2. (A) Right TPJ activation showed greater activation in the control group than the premutation group in the contrast of TWM retrieval > SWM retrieval (MNI coordinates (*x*,*y*,*z*): 52, −38, 22). (B) Beta coefficients in the right TPJ in neurotypical and premutation groups in the retrieval phase of each WM task. Only the neurotypical group showed significant enhancement of activation in the right TPJ during TWM retrieval than SWM retrieval, while such selective enhancement in the right TPJ for temporal processing was absent in the premutation group.

that only the control group showed significantly enhanced activation in the right TPJ in the TWM condition compared to the SWM condition, $t(17) = 3.02$, $p = .008$. Finally, the control group revealed significantly greater activation in the right TPJ than the premutation group during TWM retrieval, $t(34) = 2.06$, $p = .047$, whereas such differences were not found during SWM retrieval, $t(34) = .66$, $p = .52$. Unlike the right TPJ activation, results from the left posterior cingulate and left middle temporal gyrus revealed that significant activation in the group contrast map was actually driven by deactivation in the area rather than activation. In short, these results support our hypothesis that premutation carriers fail to show enhanced activation in the *when* pathway during retrieval of temporal order information than spatial location, while neurotypical adults without the premutation allele activate the right TPJ to a greater extent during TWM retrieval than SWM retrieval.

3.2.2. Multiple regression analysis using FMR1 gene expressions

Results from the multiple regression analysis indicated that *FMR1* genetic factors can account for a significant amount of variance in the right TPJ activation in the premutation group ($R^2 = .42$, $F(2,14) = 4.99$, $p = .023$). Further, the analysis showed that *FMR1* mRNA level was the most significant predictor of activation in the right TPJ. That is, we found a significant negative correlation between mRNA level and the right TPJ activation associated with temporal processing in premutation carriers ($r = -.64$, $p = .006$, two-tailed, significant after correction for multiple comparisons), and the effect remained significant even after controlling out the effect of CGG repeat size on the activation ($r_p = -.54$, $\beta = -.59$, $p = .029$). In contrast, an effect of CGG repeat size on the right TPJ activation was not significant before and after ruling out the effect of *FMR1* mRNA level ($r = -.43$, $p = .075$, two-tailed, and $rp = -.10$, $\beta = -.09$, $p = .71$, respectively). Overall, the results from the regression analysis suggest that the elevated *FMR1* mRNA level is a critical factor for reduced involvement of the *when* pathway in adults with the FX premutation during retrieval of temporal order information.

4. Discussion

The current study is the first to use fMRI to identify altered brain activity associated with temporal processing in asymptomatic adults with the FX premutation. Using two similar WM tasks, separately tagging spatial (SWM) and temporal (TWM) processing, we found that adults with the FX premutation took a significantly longer time to retrieve temporal order information than to retrieve spatial information, suggesting relative inefficiency in processing temporal order information in premutation carriers. In addition to this novel behavioral finding, we also demonstrate altered neural correlates of temporal processing in asymptomatic young adults with the FX premutation. Using the subtraction paradigm in fMRI analysis, we replicated activation in the *when* pathway in our neurotypical controls associated with temporal processing, which encompasses the right TPJ, angular gyrus, supramarginal gyrus and the posterior superior temporal gyrus [19]. By contrast, premutation carriers failed to show significant activation in the *when* pathway of the right parietal lobe in the same contrast (TWM retrieval > SWM retrieval). Further, attenuated neural activity in the right TPJ associated with the temporal processing was significantly accounted for by the elevated level of *FMR1* mRNA in premutation carriers after accounting for the effect of CGG repeat size on the activation.

The current finding of relatively inefficient temporal processing in FX premutation carriers is consistent with the previous finding from our group on impaired temporal resolution of attention in infants with FXS [4]. In the previous study, the authors found that infants with FXS showed a significantly coarser resolution of temporal attention than typically developing infants, indicating a selective impairment in temporal visual attention in infants with FXS. It is important to note that the pathology of the FX full mutation may differ from that of the FX premutation, as the former leads to intellectual disability due to a lack of FMRP expression and the latter is associated with a neurodegenerative disorder (i.e., FXTAS). In spite of this difference, our finding of inefficiency in temporal order processing in premutation carriers further supports the hypothesis that temporal processing impairments are present in individuals on the FX spectrum that resembles in a milder form that seen in the full mutation. Further, the inefficiency of retrieving temporal order information might be the developmental consequence of reduced resolution for temporal information that can be detected in infancy. Future research examining the temporal processing abilities of infants or young children with the FX premutation would be fruitful in elucidating the developmental aspects of temporal processing in FX premutation carriers.

Here, we report a novel finding that adults with the FX premutation failed to show increased involvement of the *when* pathway of the right TPJ during retrieval of temporal information compared to retrieval of spatial information. It is noteworthy that control adults without the premutation allele activated bilateral parietal areas in response to the temporal order processing in our contrast of interest. Although lesion and TMS studies have indicated that the *when* pathway is lateralized in the right parietal lobe, particularly involving the right TPJ [19–21], a recent fMRI study reported significant activation in the left TPJ associated with temporal order judgments [22]. Specifically, Davis and colleagues (2009) demonstrated strong activation in bilateral TPJ when individuals make temporal order judgments than when they make shape judgments, and also found significant left TPJ activation in the same contrast when they controlled out the effect of stimulus onset in their tasks. Thus, a conclusion of whether the *when* pathway in the parietal lobe is right lateralized or involves bilateral TPJ requires further investigation. Nonetheless, in the current study, we demonstrate that FX premutation carriers failed to show significant activation in the right TPJ for temporal order processing, as was shown by their neurotypical counterparts. In addition, activation found in the left parietal lobe in the control group in our study did not include left TPJ activation. Thus, it is likely that our results are in line with the findings from lesion and TMS studies suggesting that the right TPJ, in particular, is the key region for the *when* pathway [19–21], though more definitive studies are needed for this conclusion to be made definitively.

Importantly, not only did we find significantly attenuated right TPJ activation associated with the temporal processing in adults with the premutation, but also we found a dosage effect of *FMR1* gene expression on the altered right TPJ activation in premutation carriers. Specifically, using a multiple regression analysis, we demonstrated that the elevated level of *FMR1* mRNA in premutation carriers has a significant effect on attenuated neural activity in the right TPJ associated with the temporal processing after accounting for the effect of CGG repeat size on the activation. Recently, animal studies have reported a significant relationship between the increased CGG repeat size and impaired sequential temporal order processing in CGG KI mice modeling the FX premutation [12–14]. As opposed to findings from animal models of the FX premutation, we did not find significant modulation of CGG repeat length on altered neural activity for temporal processing in FX premutation carriers. Instead, our findings indicate that increased *FMR1* mRNA level is responsible for atypical brain activity associated with temporal order processing in the carriers. An alternative explanation for the differences between the current study and the previous animal studies may relate to *FMR1* mRNA. Because the *FMR1* mRNA level was not quantified in CGG KI mice in previous studies, the relation between the mRNA level and performance

in spatiotemporal processing tasks was underdetermined. Hence, our findings add to the animal literature by providing additional evidence that the *FMR1* mRNA level is a powerful predictor of altered temporal processing in FX premutation carriers.

The current finding showing a significant relationship between the elevated *FMR1* mRNA level and atypical neural activity for temporal processing in premutation carriers may have important implication on FXTAS. Specifically, FXTAS case has not been reported in the full mutation range of FXS, but only reported in the premutation range. Further, *FMR1* mRNA are often abnormally elevated (i.e., 2–8 times normal levels) in the FX premutation and in FXTAS. Based on these evidences, researchers have proposed a toxic gain-of-function of model for FXTAS, in which the *FMR1* mRNA itself is causative of this neurodegenerative disorder [7,10,32,33]. Moreover, there has been evidence on the significant relationship of the elevated *FMR1* mRNA level with neural changes in brain areas in men with FXTAS [34], as well as with increased psychological symptoms in adult male premutation carriers with and without FXTAS [35]. Therefore, the significant relationship between the elevated *FMR1* mRNA level and atypical brain activity in the *when* pathway found in the current study could indicate presymptomatic brain changes associated with FXTAS, although the current study does not directly address the role of *FMR1* mRNA in the pathogenesis of FXTAS. Future studies with longitudinal data including patients with FXTAS could clarify whether the association between the elevated *FMR1* mRNA level and aberrant right TPJ activation for temporal processing in premutation carriers is a prodrome of FXTAS or is a phenomenon associated with the premutation in general.

Although the current study provides novel evidence on altered neural correlates of temporal processing in asymptomatic adults with the FX premutation, some limitations of the present study need to be addressed. First, our experiments are purposely designed to find neural correlates that are particularly associated with temporal processing. For our purpose, we designed our two WM tasks separately tagging spatial and temporal processing (SWM task and TWM task, respectively). Although we tried to minimize the load for retrieving spatial information in our TWM task by providing cues (i.e., bolded lines) for all of the pre-occupied locations at retrieval, we cannot perfectly rule out the possibility of participants' strategy to memorize spatial location accompanied with temporal order when they were encoding information in the TWM task. Thus, whereas our SWM task can serve as a proper 'control' task for the TWM task to be used in the subtraction paradigm in fMRI analysis, the TWM task might not be the best control task for the SWM task per se as the TWM task may possibly impose memory loads for spatial location for some participants. In fact, in the contrast of SWM retrieval > TWM retrieval, no significant clusters in the brain was found in either diagnostic group, despite the fact that task performance indexed by the accuracy scores were somewhat lower in the SWM than the TWM task in both groups. A future study with a control task for the SWM task, such as a WM task for color information without spatial features, could provide evidence on whether or not neural substrates of spatial processing itself are also altered in non-FXTAS premutation carriers. Second, it is important to point out that the measures of CGG repeat size and *FMR1* mRNA were ascertained from blood samples and may not necessarily reflect what would be found in brain tissue. Although inter-tissue somatic stability of CGG repeat size has been demonstrated, studies have reported that *FMR1* mRNA expression varies across tissue type and between different brain regions [36]. Finally, although the results from our multiple regression analysis suggest an important role of *FMR1* mRNA on the atypical involvement of the *when* pathway for temporal processing in premutation carriers over the effect of CGG repeat size, absence of FMRP data in our study opens the possibility of a significant role of FMRP on the altered brain function for temporal processing in the premutation. Future research with direct FMRP measurement could add important knowledge on primary genetic factors on impaired temporal processing in individuals with the FX premutation.

In summary, the current study demonstrates dysfunctions in the *when* pathway, particularly the right TPJ, associated with temporal processing in asymptomatic adults with the FX premutation. Our findings expand previous findings on temporal processing deficits in infants with FXS, by providing the first evidence that neural correlates of temporal processing is altered in premutation carriers, which are *FMR1* genetic dosage sensitive indexed by *FMR1* mRNA level. Though further investigation with FMRP and patients with FXTAS are necessitated, our findings may suggest a mild form of RNA toxicity on neural substrates of temporal processing in premutation carriers that in some may progress to a related neurodegenerative disorder, FXTAS, later in life.

Acknowledgments

This research was supported by NIH grants RL1NS062412, TL1DA024854, and UL1DE019583. We would like to thank Yingratana Bella McLennan and Ling Wong for help with data collection.

References

[1] Farzin F, Rivera SM, Whitney D. Time crawls: the temporal resolution of infants' visual attention. Psychological Science 2011;22(8):1004–10.
[2] Battelli L, Cavanagh P, Intriligator J, Tramo MJ, Henaff MA, Michel F, et al. Unilateral right parietal damage leads to bilateral deficit for high-level motion. Neuron 2001;32(6):985–95.
[3] Verstraten FA, Cavanagh P, Labianca AT. Limits of attentive tracking reveal temporal properties of attention. Vision Research 2000;40(26):3651–64.
[4] Farzin F, Rivera SM, Whitney D. Resolution of spatial and temporal visual attention in infants with fragile X syndrome. Brain: A Journal of Neurology 2011;134(Pt 11):3355–68.
[5] Hagerman RJ, Berry-Kravis E, Kaufmann WE, Ono MY, Tartaglia N, Lachiewicz A, et al. Advances in the treatment of fragile X syndrome. Pediatrics 2009;123(1):378–90.
[6] Garcia-Arocena D, Hagerman PJ. Advances in understanding the molecular basis of FXTAS. Human Molecular Genetics 2010;19(R1):R83–9.
[7] Hagerman PJ, Hagerman RJ. The fragile-X premutation: a maturing perspective. American Journal of Human Genetics 2004;74(5):805–16.
[8] Kenneson A, Zhang F, Hagedorn CH, Warren ST. Reduced FMRP and increased FMR1 transcription is proportionally associated with CGG repeat number in intermediate-length and premutation carriers. Human Molecular Genetics 2001;10(14):1449–54.
[9] Tassone F, Hagerman RJ, Taylor AK, Gane LW, Godfrey TE, Hagerman PJ. Elevated levels of FMR1 mRNA in carrier males: a new mechanism of involvement in the fragile-X syndrome. American Journal of Human Genetics 2000;66(1):6–15.
[10] Hagerman RJ, Leehey M, Heinrichs W, Tassone F, Wilson R, Hills J, et al. Intention tremor, Parkinsonism, and generalized brain atrophy in male carriers of fragile X. Neurology 2001;57(1):127–30.
[11] Jacquemont S, Hagerman RJ, Leehey MA, Hall DA, Levine RA, Brunberg JA, et al. Penetrance of the fragile X-associated tremor/ataxia syndrome in a premutation carrier population. JAMA: The Journal of the American Medical Association 2004;291(4):460–9.
[12] Borthwell RM, Hunsaker MR, Willemsen R, Berman RF. Spatiotemporal processing deficits in female CGG KI mice modeling the fragile X premutation. Behavioural Brain Research 2012;233(1):29–34.
[13] Hunsaker MR, Goodrich-Hunsaker NJ, Willemsen R, Berman RF. Temporal ordering deficits in female CGG KI mice heterozygous for the fragile X premutation. Behavioural Brain Research 2010;213(2):263–8.
[14] Hunsaker MR, Kim K, Willemsen R, Berman RF. CGG trinucleotide repeat length modulates neural plasticity and spatiotemporal processing in a mouse model of the fragile X premutation. Hippocampus 2012;22(12):2260–75.
[15] Keri S, Benedek G. Why is vision impaired in fragile X premutation carriers? The role of fragile X mental retardation protein and potential FMR1 mRNA toxicity. Neuroscience 2012;206:183–9.
[16] Keri S, Benedek G. Visual pathway deficit in female fragile X premutation carriers: a potential endophenotype. Brain and Cognition 2009;69(2):291–5.
[17] Hocking DR, Kogan CS, Cornish KM. Selective spatial processing deficits in an at-risk subgroup of the fragile X premutation. Brain and Cognition 2012;79(1):39–44.
[18] Wong LM, Goodrich-Hunsaker NJ, McLennan Y, Tassone F, Harvey D, Rivera SM, et al. Young adult male carriers of the fragile X premutation exhibit genetically modulated impairments in visuospatial tasks controlled for psychomotor speed. Journal of Neurodevelopmental Disorders 2012;4(1):26.

[19] Battelli L, Pascual-Leone A, Cavanagh P. The 'when' pathway of the right parietal lobe. Trends in Cognitive Sciences 2007;11(5):204–10.
[20] Battelli L, Walsh V, Pascual-Leone A, Cavanagh P. The 'when' parietal pathway explored by lesion studies. Current Opinion in Neurobiology 2008;18(2):120–6.
[21] Woo SH, Kim KH, Lee KM. The role of the right posterior parietal cortex in temporal order judgment. Brain and Cognition 2009;69(2):337–43.
[22] Davis B, Christie J, Rorden C. Temporal order judgments activate temporal parietal junction. The Journal of Neuroscience: The Official Journal of the Society for Neuroscience 2009;29(10):3182–8.
[23] Wechsler D. WAIS-III administration and scoring manual. San Antonio, TX: The Psychological Corporation; 1997.
[24] Tassone F, Hagerman RJ, Chamberlain WD, Hagerman PJ. Transcription of the FMR1 gene in individuals with fragile X syndrome. American Journal of Medical Genetics 2000;97(3):195–203.
[25] Allen EG, Sherman S, Abramowitz A, Leslie M, Novak G, Rusin M, et al. Examination of the effect of the polymorphic CGG repeat in the FMR1 gene on cognitive performance. Behavior Genetics 2005;35(4):435–45.
[26] Tassone F, Pan R, Amiri K, Taylor AK, Hagerman PJ. A rapid polymerase chain reaction-based screening method for identification of all expanded alleles of the fragile X (FMR1) gene in newborn and high-risk populations. The Journal of Molecular Diagnostics: JMD 2008;10(1):43–94.
[27] Hashimoto R, Lee K, Preus A, McCarley RW, Wible CG. An fMRI study of functional abnormalities in the verbal working memory system and the relationship to clinical symptoms in chronic schizophrenia. Cerebral Cortex 2010;20(1):46–60.
[28] Fiebach CJ, Rissman J, D'Esposito M. Modulation of inferotemporal cortex activation during verbal working memory maintenance. Neuron 2006;51(2):251–61.
[29] Buchsbaum BR, Olsen RK, Koch P, Berman KF. Human dorsal and ventral auditory streams subserve rehearsal-based and echoic processes during verbal working memory. Neuron 2005;48:687–97.
[30] Zarahn E, Aguirre G, D'Esposito M. A trial-based experimental design for fMRI. NeuroImage 1997;6:122–38.
[31] Poline JB, Worsley KJ, Evans AC, Friston KJ. Combining spatial extent and peak intensity to test for activations in functional imaging. NeuroImage 1997;5(2):83–96.
[32] Jacquemont S, Hagerman RJ, Leehey M, Grigsby J, Zhang L, Brunberg JA, et al. Fragile X premutation tremor/ataxia syndrome: molecular, clinical, and neuroimaging correlates. American Journal f Human Genetics 2003;72(4):869–78.
[33] Greco CM, Hagerman RJ, Tassone F, Chudley AE, Del Bigio MR, Jacquemont S, et al. Neuronal intranuclear inclusions in a new cerebellar tremor/ataxia syndrome among fragile X carriers. Brain: A Journal of Neurology 2002;125(Pt 8):1760–71.
[34] Greco CM, Berman RF, Martin RM, Tassone F, Schwartz PH, Chang A, et al. Neuropathology of fragile X-associated tremor/ataxia syndrome (FXTAS). Brain: A Journal of Neurology 2006;129(Pt 1):243–55.
[35] Hessl D, Tassone F, Loesch DZ, Berry-Kravis E, Leehey MA, Gane LW, et al. Abnormal elevation of FMR1 mRNA is associated with psychological symptoms in individuals with the fragile X premutation. American journal of medical genetics Part B: Neuropsychiatric genetics: the Official Publication of the International Society of Psychiatric Genetics 2005;139B(1):115–21.
[36] Tassone F, Iwahashi C, Hagerman PJ. FMR1 RNA within the intranuclear inclusions of fragile X-associated tremor/ataxia syndrome (FXTAS). RNA Biology 2004;1(2):103–5.